Monthly Notices
of the
ROYAL ASTRONOMICAL SOCIETY

MNRAS **490,** 2421–2429 (2019)
Advance Access publication 2019 October 9

doi:10.1093/mnras/stz2800

The contribution of Centaur-emitted dust to the interplanetary dust distribution

A. R. Poppe ★

Space Sciences Laboratory, University of California at Berkeley, Berkeley, CA 94720, USA

Accepted 2019 October 1. Received 2019 September 13; in original form 2019 July 29

ABSTRACT

Interplanetary dust grains originate from a variety of source bodies, including comets, asteroids, and Edgeworth–Kuiper belt objects. Centaurs, generally defined as those objects with orbits that cross the outer planets, have occasionally been observed to exhibit cometary-like outgassing at distances beyond Jupiter, implying that they may be an important source of dust grains in the outer Solar system. Here, we use an interplanetary dust grain dynamics model to study the behaviour and equilibrium distribution of Centaur-emitted interplanetary dust grains. We focus on the five Centaurs with the highest current mass-loss rates: 29P/Schwassmann-Wachmann 1, 166P/2001 T4, 174P/Echeclus, C/2001 M10, and P/2004 A1, which together comprise 98 per cent of the current mass loss from all Centaurs. Our simulations show that Centaur-emitted dust grains with radii $s < 2$ μm have median lifetimes consistent with Poynting–Robertson (P–R) drag lifetimes, while grains with radii $s > 2$ μm have median lifetimes much shorter than their P–R drag lifetimes, suggesting that dynamical interactions with the outer planets are effective in scattering larger grains, in analogy to the relatively short lifetimes of Centaurs themselves. Equilibrium density distributions of grains emitted from specific Centaurs show a variety of structure including local maxima in the outer Solar system and azimuthal asymmetries, depending on the orbital elements of the parent Centaur. Finally, we compare the total Centaur interplanetary dust density to dust produced from Edgeworth–Kuiper belt objects, Jupiter-family comets, and Oort cloud comets, and conclude that Centaur-emitted dust may be an important component between 5 and 15 au, contributing approximately 25 per cent of the local interplanetary dust density at Saturn.

Key words: meteorites, meteors, meteoroids – minor planets, asteroids: individual: Centaurs – zodiacal dust.

1 INTRODUCTION

The production of interplanetary dust grains with sizes between ∼0.1 μm and 1 mm arises from mutual collisions, cometary outgassing, and interplanetary and interstellar meteoroid bombardment of various minor Solar system bodies. These bodies include asteroids, comets [including both short-period Jupiter-family and long-period Halley-type and Oort cloud comets (OCC)], and Edgeworth–Kuiper belt (EKB) objects. The relative contributions of each of these parent body sources to the equilibrium interplanetary dust grain distribution have been quantified through both *in situ* (e.g. Humes 1980; Grün et al. 1997; Dikarev & Grün 2002; Landgraf et al. 2002; Poppe et al. 2010; Szalay, Piquette & Horányi 2013; Malaspina et al. 2014; Piquette et al. 2019) and remote sensing observations (e.g. Hanner et al. 1974; Kelsall et al. 1998; Hahn et al. 2002; Brown et al. 2008; Campbell-Brown 2008), as well as via comparison to dynamical models (e.g. Landgraf et al. 2002; Nesvorný et al. 2010; Han et al. 2011; Vitense et al. 2012; Rowan-Robinson & May 2013; Poppe 2016; Poppe et al. 2019).

Among the various classes of minor bodies in the Solar system, the Centaurs represent a highly dynamic and relatively unstable population. Centaurs are generally defined as objects whose perihelia and semimajor axes are within the semimajor axes of Jupiter (a_J = 5.2 au) and Neptune (a_N = 30.0 au) and thus, experience relatively frequent encounters with the outer planets. (Note that Jupiter trojans are typically omitted from the designation of Centaurs, as most Trojans have $q < a_J$.) Dynamical simulations suggest that Centaurs are sourced from the scattered disc of EKB objects and following a stochastic series of encounters with the outer planets, can either be injected into Jupiter-family cometary orbits or ejected from the Solar system completely, with dynamical lifetimes ranging from 10^5 to 10^7 yr (e.g. Levison & Duncan 1997; Tiscareno & Malhotra 2003; Horner, Evans & Bailey 2004; Di Sisto & Brunini 2007; Bailey &

★ E-mail: poppe@berkeley.edu

© 2019 The Author(s)
Published by Oxford University Press on behalf of the Royal Astronomical Society

Downloaded from https://academic.oup.com/mnras/article-abstract/490/2/2421/5584353 by University of California School of Law (Boalt Hall) user on 29 October 2019

Malhotra 2009; Volk & Malhotra 2013). Centaurs thus represent a link between the distant, quiescent EKB and the volatilized outgassing and disruption seen in the Jupiter-family comets (JFC).

Interestingly, despite their distance beyond the sublimation point of water ice (which drives the behaviour of typical inner Solar system comets), a fraction of Centaurs have been observed to undergo cometary-like outgassing (e.g. Hartmann, Tholen & Meech 1990; Mazzotta Epifani et al. 2011, 2014, 2017; Kulyk et al. 2016) of both steady and episodic nature. Jewitt (2009) compiled an extensive set of observations of 23 Centaurs, of which nine displayed detectable comae due to active outgassing. Calculations of the mass-loss rates from these 'active' Centaurs ranged from 10^1 up to 10^3 kg s^{-1} (the lattermost rate for the well-known Centaur 29P/Schwassmann-Wachmann 1). This activity is most likely not driven by sublimation of crystalline water ice (which would occur at much lower heliocentric distances) but rather by the conversion of amorphous water ice into its crystalline form, thereby releasing trapped gases that then entrain and accelerate dust grains away from the object (e.g. Jewitt 2009; Meech et al. 2009). Thus, outgassing and dust grain loss from Centaurs could be an important source of interplanetary dust grains in the outer Solar system. Indeed, Landgraf et al. (2002) modelled the dynamics of 5 and 10 μm radius dust grains produced from 29P/Schwassmann-Wachmann 1, compared these results to Pioneer 10 and 11 *in situ* measurements of Humes (1980), and suggested that 29P could alone be responsible for a large fraction of dust inside the orbit of Saturn.

A quantification of interplanetary dust grain sources is critical to understanding a variety of physical processes in the outer Solar system. For example, interplanetary dust grains can contribute exogenous material to the atmospheres of the outer planets and Titan thereby altering both atmospheric photochemistry (e.g. English et al. 1996; Feuchtgruber et al. 1999; Moses et al. 2000; Cavalié et al. 2014; Frankland et al. 2016; Moses and Poppe 2017) and ionospheric structure and composition (e.g. Lyons 1995; Moses & Bass 2000; Petrie 2004). An influx of interplanetary dust grains is also thought to play an important role in both 'polluting' the main ring system of Saturn with dark, exogenous materials and modifying the radial distribution of mass and angular momentum within the rings (e.g. Durisen et al. 1989, 1992, 1996; Poulet & Cuzzi 2002; Estrada et al. 2015). The formation of tenuous rings at all four of the outer planets, including, for example, the inner rings of Jupiter (e.g. Burns et al. 1999) and the extended Phoebe ring at Saturn (Verbiscer, Skrutskie & Hamilton 2009), and the formation of tenuous 'dust exospheres' at the Galilean satellites (e.g. Krüger et al. 1999; Krüger, Krivov & Grün 2000; Sremčević et al. 2005), are all governed by bombardment of small satellites by interplanetary dust grains.

Here, we use the observations of Centaur mass-loss rates by Jewitt (2009) and the dynamical dust grain model of Poppe (2016) to quantify the dynamics and equilibrium distributions of Centaur-emitted dust grains. In Section 2, we summarize the observations of active Centaurs and calculate the relevant dust grain production rates. In Section 3, we present results from the dynamical dust grain model for Centaur-emitted dust, including the distribution of Centaur-emitted grain lifetimes, equilibrium density distributions, and comparisons to other dominant interplanetary dust grain sources. Finally, we discuss our results and conclude in Section 4.

2 DUST PRODUCTION ESTIMATES FROM CENTAURS

Since the discovery of the first Centaur object, (2060) Chiron (Kowal, Liller & Marsden 1979), decades of observations have now identified 263 objects that meet the criteria used here ($5.2 < [q, a] < 30.01$) for classification as a Centaur.[1] Observations have furthermore established that a subset of these objects shows cometary-like activity at distances beyond that considered 'typical' for a comet (e.g. Hartmann et al. 1990; Bauer, Fernández & Meech 2003; Bauer et al. 2008; Jewitt 2009; Mazzotta Epifani et al. 2011, 2014; Hosek et al. 2013; Kulyk et al. 2016). In particular, Jewitt (2009) reported observations of nine active Centaurs among a population of 23 observed (or ∼40 per cent, although we note that the selection of Centaurs observed by Jewitt 2009 is by design most likely biased in favour of active objects). The active Centaur group was also observed to have a lower median perihelion distance of 5.9 au compared to the median perihelion distance of inactive Centaurs of 8.7 au. Of the nine observed active Centaurs, mass production rates for dust grains with radii between 0.1 μm and 1 cm ranged from 4.3 kg s^{-1} (39P/Oterma) up to 5.1×10^3 kg s^{-1} (29P/Schwassmann-Wachmann 1). For our study, we identified the five Centaurs with the highest mass-loss rates: 29P/Schwassmann-Wachmann 1, 166P/2001 T4, 174P/Echeclus, C/2001 M10, and P/2004 A1. Taken together, these five objects comprise ∼98 per cent of the total observed mass-loss rate from the nine active Centaurs observed by Jewitt (2009).

Table 1 lists the characteristics of the five Centaurs studied here, including the perihelion distance, q, semimajor axis, a, aphelion distance, Q, eccentricity, e, inclination, i, argument of pericentre, ω, and longitude of ascending node, Ω. Furthermore, we also list the 0.1 μm–1 cm dust production rate, $\dot{M}$, from Jewitt (2009). Previous theoretical and computational modelling of interplanetary dust grain production has more often cited production rates over sizes ranges from 0.1 to 10 μm (e.g. Stern 1996; Yamamoto & Mukai 1998; Han et al. 2011; Poppe 2016) and thus, to more directly compare with previous work, we assume a power-law distribution for the mass production of dust grains given by $\mathrm{d}\dot{M}/\mathrm{d}m \propto m^{-\alpha/3}$, where $\alpha = 2.5$ (e.g. Dohnanyi 1969), and calculate the mass production rate strictly between 0.1 and 10 μm, defined as $\dot{M}'$. One can see from Table 1 that the dominant dust-producing Centaur is 29P/Schwassmann-Wachmann 1, with 80.0 per cent of the total. The following four Centaurs (166P, 174P, C/2001 M10, P/2004 A1) all produce smaller amounts of dust than 29P (around 3–5 per cent of total each). The remaining active Centaurs not selected here for study account for the final 2 per cent of total Centaur-emitted dust.

Fig. 1 shows the orbits of the five selected Centaurs (coloured lines) projected down on to the ecliptic plane with the orbits of the outer planets as well (grey lines). Different types of orbits exist even among these five selected Centaurs: 29P/Schwassmann-Wachmann 1 is on a nearly circular orbit ($e = 0.045$) just outside the orbit of Jupiter; 166P, 174P, and P/2004 A1 have moderate eccentricities ($e \sim 0.3$–0.45) and cross the orbits of Saturn and Uranus (the latter in the case of 166P); and C/2001 M10 is on a highly eccentric orbit ($e = 0.801$) and crosses the orbits of all four outer planets (Jupiter's aphelion at 5.45 au lies just outside the perihelion of C/2001 M10 at 5.30 au). We again note that the orbits of Centaurs are highly dynamic and/or chaotic. For example, Hahn et al. (2006) showed that P/2004 A1 suffered a close approach to Saturn in 1992 that lowered its semimajor axis from 12.2 to 7.91 au and that it will undergo a close approach to Jupiter in 2026 that will further lower its semimajor axis to 6.49 au. Numerical simulations of the orbit of 29P show that despite its current low-eccentricity orbit, it is in fact in a chaotic regime and most likely

[1] As of 2019 June 1 from the Minor Planet Center list.

Downloaded from https://academic.oup.com/mnras/article-abstract/490/2/2421/5584353 by University of California School of Law (Boalt Hall) user on 29 October 2019

Table 1. The list of Centaurs studied here, including their orbital elements (perihelion, q, semimajor axis, a, aphelion, Q, eccentricity, e, and inclination, i, argument of pericentre, ω, and longitude of ascending node, Ω) as of 2019 April 1 from the JPL/HORIZONS data base. The total dust mass-loss rate, $\dot{M}$, taken from Jewitt (2009) and the corresponding 0.1–10 μm dust mass-loss rate, $\dot{M}'$, are also listed. The final column lists the fraction amount that each Centaur contributes to the overall Centaur mass production rate.

Centaur name	q (au)	a (au)	Q (au)	e	i (°)	ω (°)	Ω (°)	$\dot{M}$ (g s^{-1})	$\dot{M}'$ (g s^{-1})	$\dot{M}/\dot{M}_{\rm tot}$
29P/S-W 1	5.72	5.99	6.26	0.045	9.39	49.05	312.6	5.1×10^6	1.5×10^5	80.0%
166P/2001 T4	8.56	13.9	19.2	0.383	15.37	321.8	64.5	3.3×10^5	9.4×10^3	5.2%
174P/Echeclus	5.82	10.7	15.6	0.456	4.34	162.9	173.3	3.2×10^5	9.1×10^3	5.0%
C/2001 M10	5.30	26.7	48.0	0.801	28.08	5.48	293.9	2.8×10^5	8.0×10^3	4.4%
P/2004 A1	5.46	7.9	10.3	0.308	10.58	20.5	125.2	2.0×10^5	5.7×10^3	3.1%

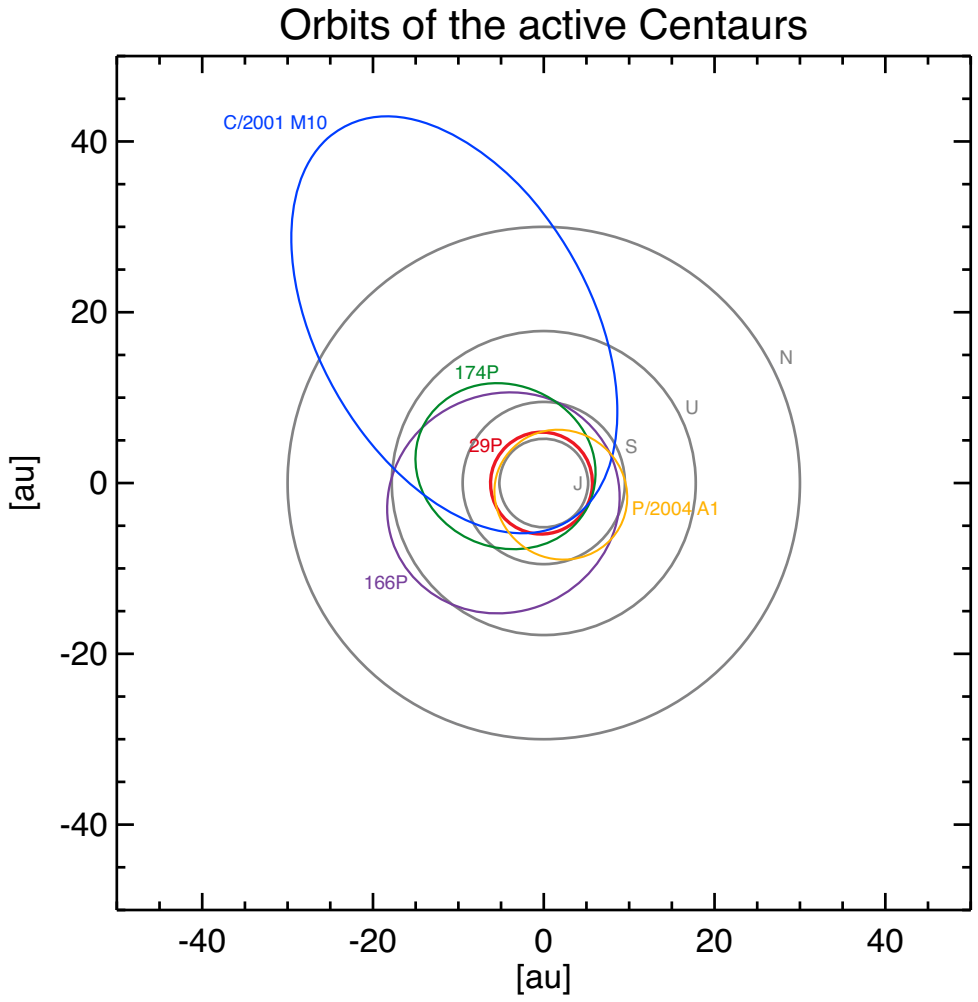

Figure 1. The orbits of the five active Centaurs selected as dust grain parent bodies for study here. Grey curves denote the orbits of the outer planets.

originated from the Oort cloud (Neslušan, Tomko & Ivanova 2017). Thus, we emphasize that our use of the current five most active Centaurs as initial conditions is, strictly speaking, only valid in today's epoch; however, we nevertheless consider current conditions at least reasonably representative of Centaur-emitted dust grain distributions over time.

Before embarking on detailed dynamical simulations, we can compare to first-order the production rates of 0.1–10 μm dust grains from Centaurs as derived here from the observations of Jewitt (2009) with constraints on the dust production rates from other dust grain sources in the Solar system. The main recognized sources of interplanetary dust grains throughout the Solar system include the asteroid belt, JFC, Halley-type comets, OCC, and EKB objects. As argued by Nesvorný et al. (2010), contributions from asteroids and Halley-type comets are at levels <10 per cent of the overall dust production in the inner Solar system and can therefore generally be neglected. Thus, JFC, OCC, and EKB grains are the primary sources with which to compare Centaur dust production rates. Recently, Poppe (2016) and Poppe et al. (2019) have employed a dynamical dust grain model along with *in situ* dust flux observations from the *Pioneer 10* meteoroid detector (Humes 1980) and the *New Horizons*/Student Dust Counter (Horányi et al. 2008; Poppe et al. 2010; Szalay et al. 2013; Piquette et al. 2019) to constrain the overall distribution of interplanetary dust and by extension, the dust

Downloaded from https://academic.oup.com/mnras/article-abstract/490/2/2421/5584353 by University of California School of Law (Boalt Hall) user on 29 October 2019

Table 2. A comparison of the dust grain production rates and approximate source regions for various interplanetary dust grain sources (Poppe et al. 2019).

Family	0.1–10 μm production rate (g s^{-1})	Approximate source region (au)
EKB	3×10^7	30–200
JFC	5×10^5	0.1–10
OCC	3×10^5	0.1–10
Centaurs	2×10^5	5–15

production rates from JFC, OCC, and EKB sources. Table 2 lists the 0.1–10 μm dust grain production rates based on the results of Poppe et al. (2019) along with the general source region (expressed as a range of heliocentric distances) for these three sources. The dominant source of dust grains are EKB objects, with a total 0.1–10 μm dust production rate of approximately 3×10^7 g s^{-1}. JFC and OCC grains are produced at rates of 5×10^5 and 3×10^5 g s^{-1}, respectively. In comparison, the total Centaur 0.1–10 μm production rate as derived from the observations of Jewitt (2009) stands at 2×10^5 g s^{-1}, nearly equal to that of the contributions from JFC and OCC sources. In some ways, this perhaps should not be so surprising, given the recognition in previous work of the fairly prodigious amount of dust generated from 29P/Schwassmann-Wachmann 1 (e.g. Fulle 1992; Landgraf et al. 2002). Nevertheless, this comparative exercise provides strong motivation to further explore and quantify the contribution of dust emitted from active Centaurs to the interplanetary dust distribution.

3 CENTAUR DUST DYNAMICS MODELLING

3.1 Model description and initial conditions

To further quantify the dynamics and equilibrium distributions of Centaur-emitted dust grains, we employed the dynamical dust grain model of Poppe (2016). This model uses a Bulirsch–Stoer integrator to track the trajectory of individual dust grains from specified initial conditions under the influence of gravitation (both solar and all eight planets), Poynting–Robertson (P–R) and solar wind drag, solar radiation pressure, and the electromagnetic Lorentz force. Dust grains are also subject to sublimation and solar wind sputtering, which can reduce the grain radius over time. Individual grains are integrated from their initial position until they are either (a) ejected from the Solar system, (b) reach a distance of 0.05 au, or (c) reach a lifetime of 10^9 yr. Modelled grain masses range from 10^{-12} to 10^{-3} g in half-logarithmic intervals (i.e. [10^{-12}, $10^{-11.5}$, ..., $10^{-3.5}$, 10^{-3}] g) that, assuming a material density of approximately 2.5 g cm^{-3}, corresponds to radii between 0.5 and 500 μm. Observations of material dust grain densities vary from 0.5 to 6.0 g cm^{-3} (e.g. Flynn & Sutton 1991; Love, Joswiak & Brownlee 1994; Fulle et al. 2015, 2017). Many of the lowest density dust grains are highly porous and are composed of aggregates of smaller elements. Variability in the material density of dust grains has implications for the dynamical behaviour of dust grains, including changes to the orbital decay due to P–R drag (e.g. Burns, Lamy & Soter 1979; Gustafson 1994), the rates of mass loss due to sputtering and sublimation (e.g. Mukai & Schwehm 1981), and the probabilities of shattering and/or destruction upon impact with other grains (e.g. Borkowski & Dwek 1995). Lower density dust grains undergo faster orbital decay due to P–R drag (since $\beta \propto 1/\rho$) and are more likely to be shattered in the event of a grain–grain collision. Our assumed material density of 2.5 g cm^{-3} lies close to the mean material density of 2.2 g cm^{-3} found in unmelted stratospheric micrometeorites by Love et al. (1994), yet is higher than that found from freshly emitted cometary dust (e.g. Fulle et al. 2015, 2017). Further discussion of the impact of material density variability is presented in Section 4. Compositionally, we assume the dust grains to be composed of general astrosilicates, which is supported by observations of ejecta from 29P (Schambeau et al. 2015) and other comets (e.g. Lisse et al. 2006, 2007). While water ice grains do exist in cometary ejecta, they will be rapidly lost due to both sublimation for heliocentric distances $<\sim$10–20 au (Kobayashi et al. 2009, 2010) and photodesorption, potentially out to much greater heliocentric distance (Grigorieva et al. 2007). Thus, we do not model icy grains here.

For each of the five modelled Centaurs, we initialized a set of dust grain state vectors using the orbital elements listed in Table 1 with true anomalies spread between [0 and 2π]. To these initial state vectors, we added an ejection velocity of 25 m s^{-1} in a randomized direction to account for the (small) deviation in trajectory due to emission drag forces acting on the grains (e.g. Jones 1995; Ma, Williams & Chen 2002). For each dust grain size and Centaur, we traced 2400 individual grains, resulting in a total number of approximately 45 000 grains for each active Centaur.

3.2 Modelling results

Fig. 2(a) shows the distribution of Centaur-emitted dust grain lifetimes as a function of grain radius. We also denote the theoretical P–R lifetime for a grain born on a circular orbit at 5 au (dashed line) and the median dynamical lifetime from the simulations (solid line), for comparison. Median Centaur grain lifetimes across nearly all grain sizes are on the order of 10^5–10^6 yr. At sizes below approximately 1 μm, the median grain lifetimes correspond reasonably well to the theoretical P–R drag lifetime, suggesting that planetary encounters play less of a role in their dynamics than does solar radiation effects. The small population of $s < 2$ μm grains with lifetimes on the order of 10^2 yr are those grains born directly on to escaping trajectories, i.e. they are classified as a form of β-meteoroids (Zook & Berg 1975; Wehry & Mann 1999). For grains with $s > 1$ μm, the theoretical P–R drag lifetimes and the median simulated lifetimes quickly diverge, with the median dynamical lifetimes never exceeding 10^6 yr. Interestingly, the median lifetime of $s > 1$ μm Centaur grains found here, $\sim 8 \times 10^5$ yr, is an order-of-magnitude smaller than the median lifetime found for Centaurs themselves from the simulations of Tiscareno & Malhotra (2003), although we do note that the initial Centaur conditions used in Tiscareno & Malhotra (2003) (e.g. see their fig. 1) have generally higher perihelia and semimajor axes than the initial conditions of the five active Centaurs used here as initial conditions for the dust grains. Perturbative forces that are relevant for dust grains (e.g. P–R and solar wind drag, Lorentz force, etc.) may accelerate the rate of planetary encounters compared to the parent Centaurs, which are not perturbed by these same forces. Finally, we note the presence of some grains with $s > 50$ μm that do survive up to 10^9 yr, at which point the simulations are terminated. Manual inspection of these long-lived orbits shows that many of them are grains that suffered planetary encounters early-on in their lifetimes and evolved on to high inclination ($i \sim 90°$) orbits, which appear to be relatively well protected from subsequent planetary encounters.

In addition to the grain lifetimes, Fig. 2(b) shows the relative fraction of Centaur-emitted grains that either (i) escaped the Solar system or (ii) drifted to <0.05 au as a function of grain size (the

Downloaded from https://academic.oup.com/mnras/article-abstract/490/2/2421/5584353 by University of California School of Law (Boalt Hall) user on 29 October 2019

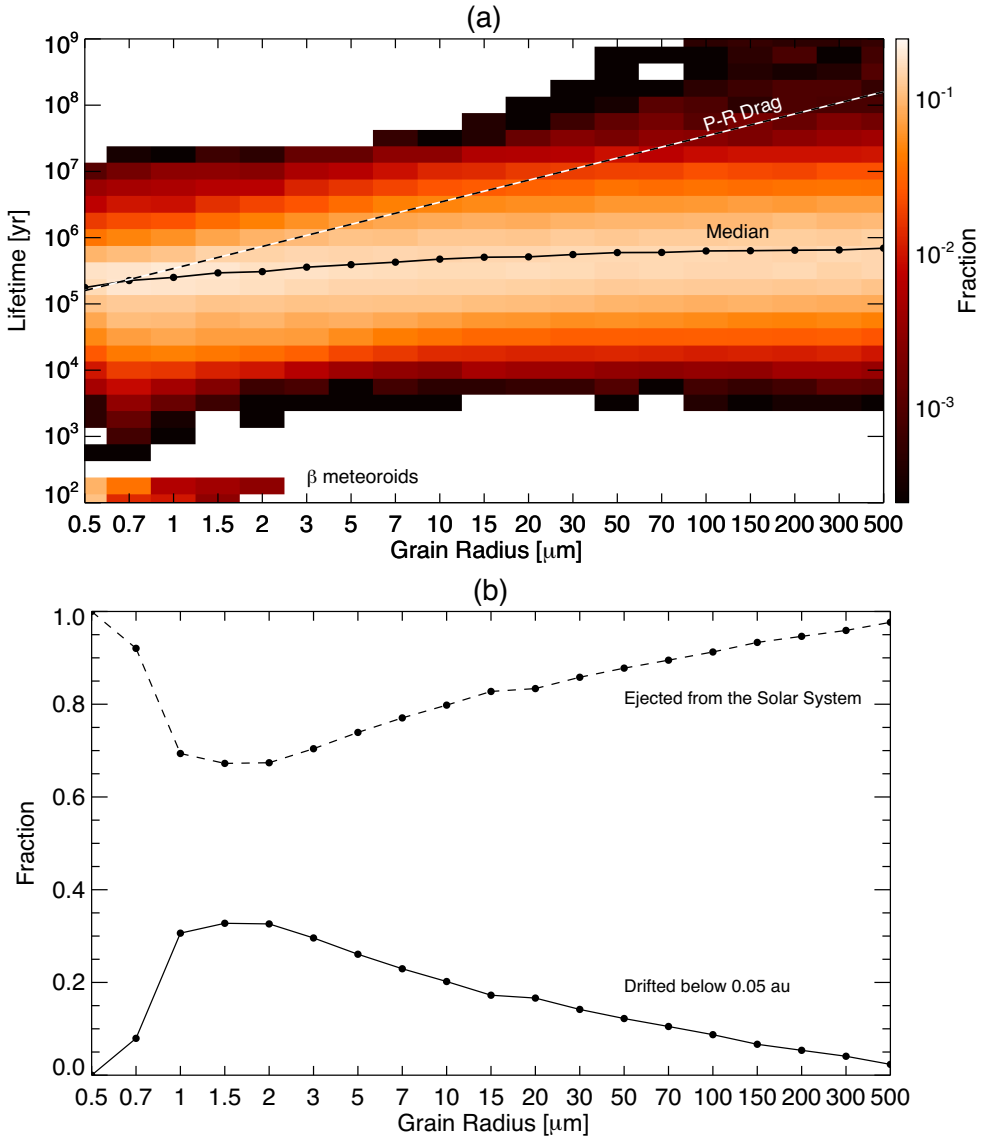

Figure 2. (a) The distribution of Centaur-emitted dust grain lifetimes as a function of grain radius. The dashed line denotes the theoretical Poynting–Robertson (P–R) drag lifetime for a grain born at 5 au on a circular orbit, for comparison. (b) The fraction of Centaur-emitted dust grains that either (i) escape the Solar system or (ii) drifted to heliocentric distances <0.05 au.

number of grains that reached lifetimes of 10^9 yr is quite small comparatively). For grains with $s > 2$ μm, an increase in grain size correlates with a higher fraction of ejection from the Solar system compared to those grains that are able to spiral into the inner Solar system. For grains with $s < 2$ μm, the curve rolls over and nearly all grains are ejected. This trend is actually not due to ejection of grains by the outer planets, as many of these smaller grains actually did indeed drift well into the inner Solar system. Instead, these grains continuously lose mass due to solar wind sputtering and/or sublimation, following which they are ejected from the Solar system by radiation pressure, i.e. they became β-meteoroids.

Fig. 3 shows the mass density of 0.5–500 μm grains in the ecliptic plane for each of the five modelled Centaurs. In each plot, we also show the projection of each Centaur's orbit on to the ecliptic plane. In Fig. 3(a), dust grains emitted from 29P/Schwassmann-Wachmann 1 are concentrated most in the inner Solar system, due to dust grains that decouple from Jupiter and drift via P–R drag through the inner Solar system. Dust emitted from 29P is also azimuthally symmetric, corresponding to the near-circular orbit of 29P itself ($e = 0.045$). The equilibrium density distributions for dust grains emitted from 166P, Fig. 3(b), 174P, Fig. 3(c), and C/2001 M10, Fig. 3(d), possess local maxima near approximately 10 au with varying degrees of azimuthal asymmetry, as well as absolute maxima in the inner Solar system. The most asymmetric distribution among these three objects is for the case of C/2001 M10, which due to the highly eccentric orbit of the parent body, yields a concentration of mass density near the argument of pericentre. The asymmetries in these cases are due to orbital element grouping of freshly emitted dust grains in direct analogy to the formation of meteoroid streams in the inner Solar system. Finally, the density distribution for grains emitted from P/2004 A1, Fig. 3(e), is similar in morphology to that of 29P, with only a single maximum in the inner Solar system and broad azimuthal symmetry.

Downloaded from https://academic.oup.com/mnras/article-abstract/490/2/2421/5584353 by University of California School of Law (Boalt Hall) user on 29 October 2019

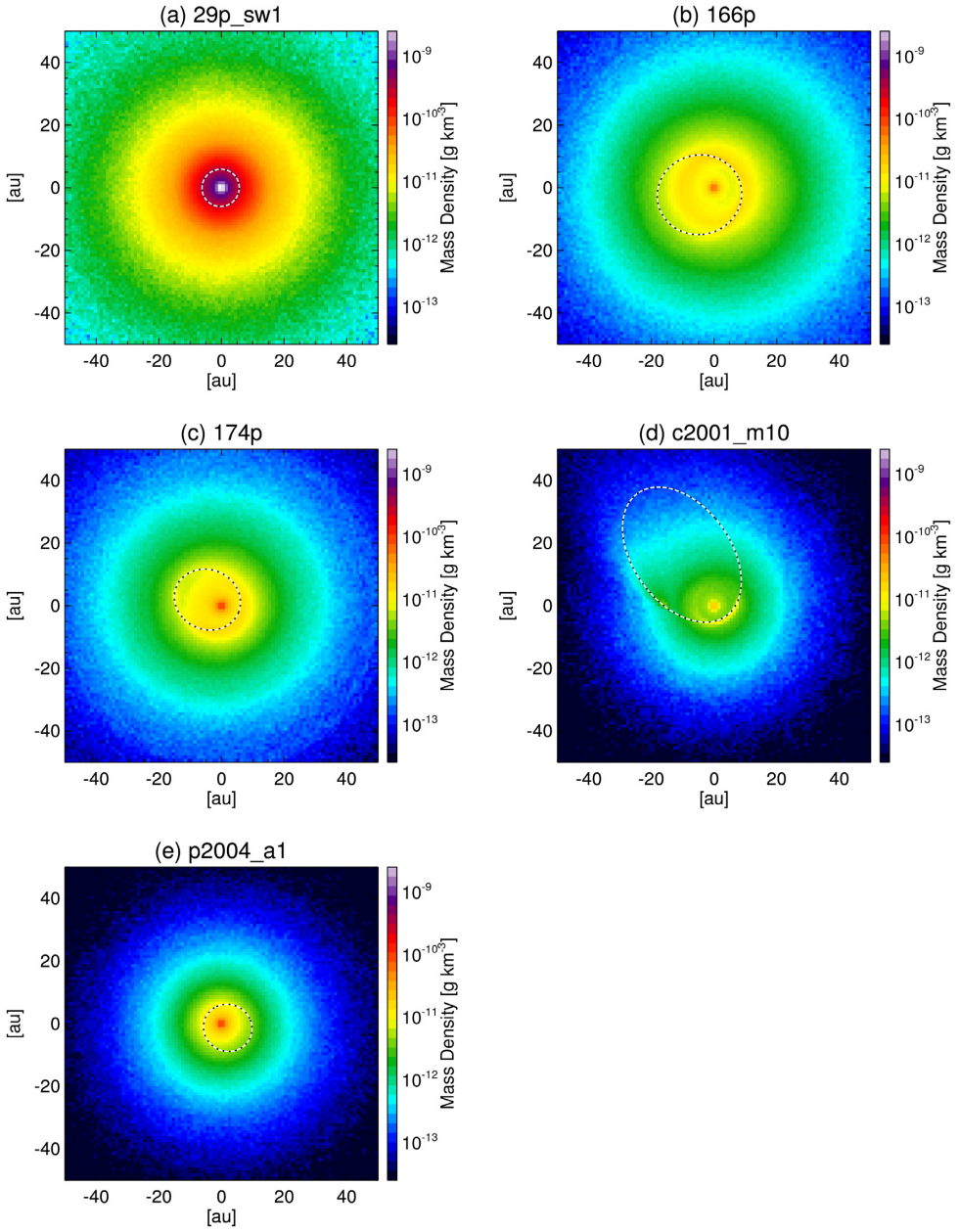

Figure 3. The equilibrium, in-ecliptic dust grain mass densities for each of the five selected active Centaurs. In each panel, the orbit of the parent Centaur is projected on to the ecliptic plane and denoted by the dotted curve.

Fig. 4 shows the azimuthally averaged, in-ecliptic absolute density and fractional density of EKB, JFC, OCC, and Centaur dust grains for four different grain sizes: (a) and (b): 0.5 μm; (c) and (d): 5 μm; (e) and (f): 50 μm; and (g) and (h): 500 μm. This comparative plot puts the contribution of Centaur-emitted dust into context with the other main interplanetary dust grain sources (e.g. Poppe 2016; Poppe et al. 2019). For 0.5 μm, Figs 4(a) and (b), EKB grains are dominant throughout nearly all of the Solar system with small exceptions near 5 au, where JFC grains are locally concentrated due to trapping in mean motion resonances with Jupiter, and within approximately 0.25 au, where JFC grains are also of equal density to EKB grains. EKB grain densities are generally flat out to approximately 40 au, beyond which densities decline. JFC 0.5 μm grains peak locally near 5 au as noted above, but rapidly fall off in density outside this peak. OCC 0.5 μm grains have densities lower than 0.5 μm JFC grains inside of ∼10 au, but have a shallower slope beyond this, thereby becoming dominant over JFC grains outside 10 au (albeit still lower than 0.5 μm EKB grains). In comparison, Centaur 0.5 μm grains are generally a minor species throughout the Solar system. Within approximately 10 au, they comprise only ∼5 per cent of the total density, while outside 10 au, they comprise at least two orders of magnitude smaller relative contribution.

The radial densities of 5, 50, and 500 μm grains follow generally the same pattern to one another. Within approximately 10 au, JFC grains are dominant and Centaur grains typically contribute between 1 and 10 per cent to the overall density. EKB and OCC 5 μm grains contribute around 10 per cent of the total within 10 au, but larger

Downloaded from https://academic.oup.com/mnras/article-abstract/490/2/2421/5584353 by University of California School of Law (Boalt Hall) user on 29 October 2019

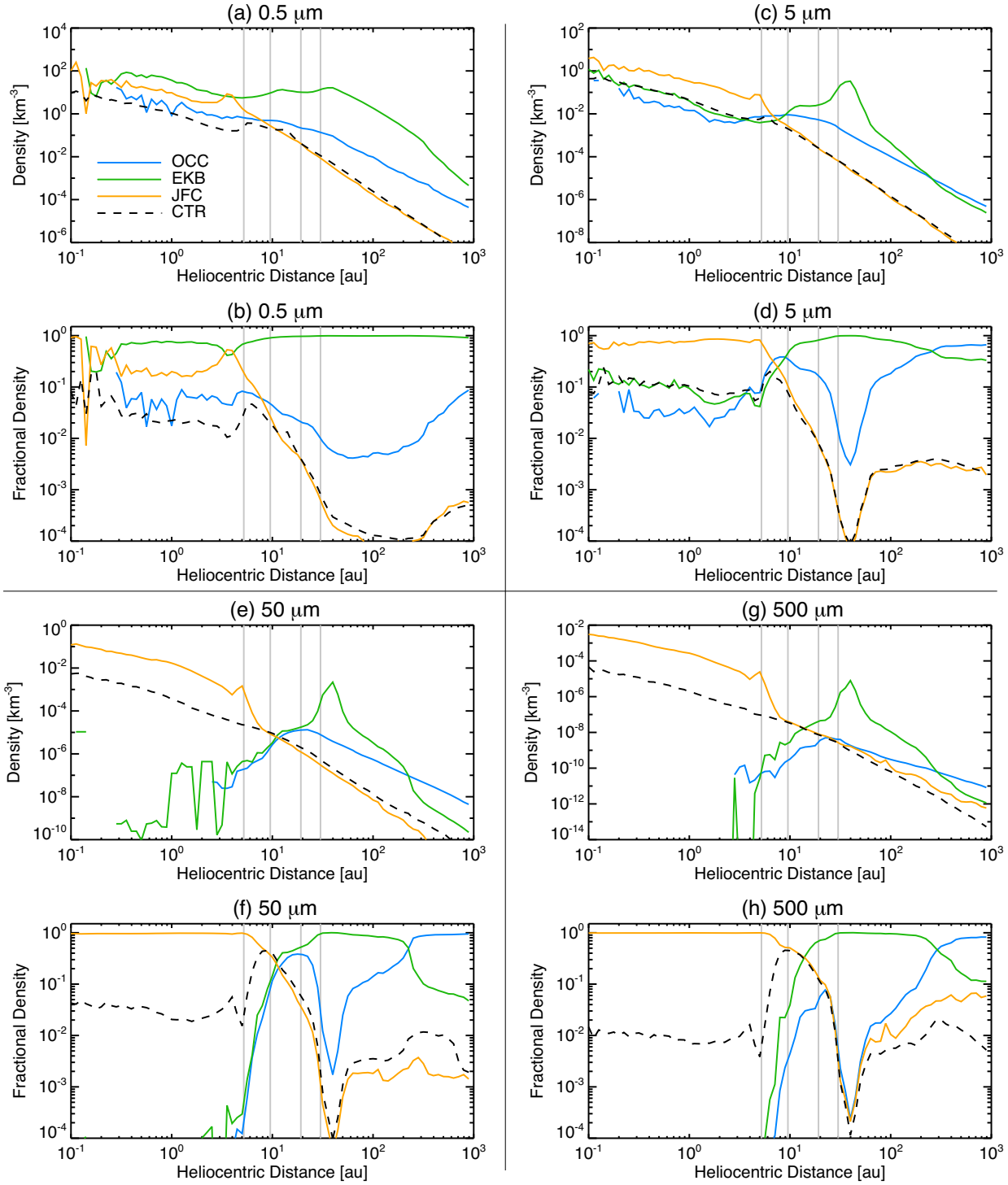

Figure 4. The in-ecliptic absolute density and fractional density as a function of heliocentric distance for four dust grain parent sources (EKB, green; OCC, blue; JFC, orange; Centaurs, dashed black) for (a) and (b) 0.5 μm, (c) and (d) 5 μm, (e) and (f) 50 μm, and (g) and (h) 500 μm radius. Vertical grey lines denote the semimajor axes of the outer planets.

sized EKB and OCC grains (50 and 500 μm) do not substantially contribute in the inner Solar system compared to JFC and Centaur grains. Near 10 au, the contributions of all four sources (including Centaur grains) to the equilibrium density are nearly equal, with only 500 μm OCC grains as an exception as they are approximately an order of magnitude less than other sources near 10 au. Between approximately 10 and 200 au, EKB grains are dominant by several orders of magnitude, reflecting the presence of the EKB parent bodies within this region (e.g. Petit et al. 2011). JFC and Centaur grains diminish much faster than the EKB grain densities and thus, do not significantly contribute to densities beyond 10–15 au. At distances beyond ∼200 au, OCC grains surpass the density of EKB

Downloaded from https://academic.oup.com/mnras/article-abstract/490/2/2421/5584353 by University of California School of Law (Boalt Hall) user on 29 October 2019

grains, which have a 'shoulder' in their density profile between approximately 200 and 400 au. Thus, the interplanetary dust grain distribution is dominated by OCC grains in the far reaches of the Solar system beyond ∼400 au.

4 DISCUSSION AND CONCLUSION

Using the known orbital elements and dust mass production rates of the active Centaurs (Jewitt 2009), we have modelled the dynamics of Centaur-emitted dust grains and quantified their potential contribution to the interplanetary dust density. From our simulations, we find that Centaur-emitted dust grains may represent an important source of interplanetary dust grains, in particular within heliocentric distances of approximately 5–15 au. We also found that dynamical lifetimes of Centaur-emitted grains can be divided into two groups: (i) grains with radii $s < 2$ μm that have lifetimes on the order of their theoretical P–R drag lifetimes and (ii) grains with radii $s > 2$ μm that have median lifetimes much shorter than their theoretical P–R drag lifetimes. The break in these two groups occurs at a lifetime between ∼200 000 and 500 000 yr, which can be interpreted as the time-scale of planetary perturbations for Centaur-emitted grains. In concordance with this, our simulations show an increasing fraction of grains ejected from the Solar system as a function of grain radius, a sure sign of planetary perturbation. Outer planet perturbations are also responsible for a population of high-inclination ($i > 60°$) Centaur-emitted grains that tend to have longer lifetimes than lower inclination grains. Variability in dust grain material densities may affect the conclusions above. In particular, grains with lower densities than assumed here ($\rho = 2.5$ g cm^{-3}) have shorter lifetimes against P–R drag and thus, will spiral into the inner Solar system faster. Thus, one would expect particles of radius larger than the 2 μm (as discussed above) to have lifetimes closer to their P–R drag time and be less susceptible to perturbation and/or ejection by the giant planets. Lower density grains may also be more likely to undergo catastrophic disruption in the event of a grain–grain collision (e.g. Borkowski & Dwek 1995), thereby reducing their spatial number density relative to that expected for higher material density grains.

Based on the equilibrium density distributions shown in Fig. 4, our modelling suggests that while Centaur-emitted dust grains are present throughout the Solar system, their most important contribution may be as a source of dust flux to the Saturnian system, on par with that expected from EKB, JFC, and OCC grains. The *Cassini* mission, in orbit around Saturn from 2004 to 2017, catalogued a wide variety of dust grains on approach to and within the Saturnian system via the *Cassini* Cosmic Dust Analyzer (CDA; Srama et al. 2004). These observations include planetary grains mainly from the E-ring sourced from Enceladus (e.g. Spahn et al. 2006; Srama et al. 2006; Kempf et al. 2008), nanometre-sized 'stream' particles accelerated away from Saturn due to electromagnetic forces (e.g. Hsu, Kempf & Jackman 2010; Hsu et al. 2011), interstellar dust (Altobelli et al. 2004, 2016), and finally, interplanetary dust (Altobelli et al. 2007; Hillier et al. 2007). Continued analysis of the *Cassini* CDA data set during its orbital tour may yield further identification of not only the interplanetary dust component, but also various subsets (e.g. EKB, JFC, OCC, and Centaurs) of the dust population expected at Saturn's orbital distance.

Finally, we note that while we have selected five specific, currently active Centaurs for our modelling here, the chaotic and relatively short-lived nature of Centaurs (Tiscareno & Malhotra 2003) implies that there is likely to be a high degree of spatial and temporal variability in the Centaur-emitted dust population. For example, our specific modelling results depend heavily on the dust emission from 29P alone (which comprises ∼80 per cent of the current total Centaur emitted dust) and thus, may be particularly sensitive to changes in 29P's orbit and instantaneous dust production rate. Temporal variability in the rate of Centaur-emitted dust grains may also sensitively depend on cases where perturbations by the outer planets cause the perihelion of a given Centaur to drop to low enough heliocentric distance to trigger the conversion of amorphous ice to crystalline ice, which has been theorized as the main mechanism underlying active Centaur emission (e.g. Jewitt 2009; Meech et al. 2009). Dust emission from Centaurs may also be expected to form collimated meteoroid streams as evidenced by azimuthally asymmetric structures seen in Fig. 3, for example; however, such streams are likely to be shorter lived than their inner Solar system counterparts due to both outer planet perturbations of the constituent meteoroid stream dust grains and of the parent Centaurs themselves.

ACKNOWLEDGEMENTS

The author acknowledges support from the NASA New Frontiers Data Analysis Program, grant #80NSSC18K1557. The author thanks B. Gladman and N. Altobelli for suggesting the topic of study, J. R. Szalay for constructive comments, and G. J. Flynn for a constructive review.

REFERENCES

Altobelli N., Dikarev V., Kempf S., Srama R., Helfert S., Moragas-Klostermeyer G., Roy M., Grün E., 2007, J. Geophys. Res., 112, 1
Altobelli N., Krüger H., Moissl R., Landgraf M., Grün E., 2004, Planet. Space Sci., 52, 1287
Altobelli N. et al., 2016, Science, 352, 312
Bailey B. L., Malhotra R., 2009, Icarus, 203, 155
Bauer J. M., Choi Y.-J., Weissman P. R., Stansberry J. A., Fernández Y. R., Roe H. G., Buratti B. J., Sung H.-I., 2008, PASP, 120, 393
Bauer J. M., Fernández Y. R., Meech K. J., 2003, PASP, 115, 981
Borkowski K. J., Dwek E., 1995, ApJ, 454, 254
Brown P., Weryk R. J., Wong D. K., Jones J., 2008, Icarus, 195, 317
Burns J. A., Lamy P. L., Soter S., 1979, Icarus, 40, 1
Burns J. A., Showalter M., Hamilton D. P., Nicholson P. D., de Pater I., Ockert-Bell M. E., Thomas P. C., 1999, Science, 284, 1146
Campbell-Brown M. D., 2008, Icarus, 196, 144
Cavalié T. et al., 2014, A&A, 562, A33
Dikarev V., Grün E., 2002, A&A, 383, 302
Di Sisto R. P., Brunini A., 2007, Icarus, 190, 224
Dohnanyi J. S., 1969, J. Geophys. Res., 74, 2531
Durisen R. H., Bode P. W., Cuzzi J. N., Cederbloom S. E., Murphy B. W., 1992, Icarus, 100, 364
Durisen R. H., Bode P. W., Dyck S. G., Cuzzi J. N., Dull J. D., White J. C., II, 1996, Icarus, 124, 220
Durisen R. H., Cramer N. L., Murphy B. W., Cuzzi J. N., Mullikin T. L., Cederbloom S. E., 1989, Icarus, 80, 136
English M. A., Lara L. M., Lorenz R. D., Ratcliff P. R., Rodrigo R., 1996, Adv. Space Res., 17, 157
Estrada P. R., Durisen R. H., Cuzzi J. N., Morgan D. A., 2015, Icarus, 252, 415
Feuchtgruber H. et al., 1999, in Cox P., Kessler M. F., eds, The Universe as Seen by ISO. ESA (ESA-SP 427), Noordwijk, p. 133
Flynn G. J., Sutton S. R., 1991, Proc. Lunar Planet. Sci., 21, 541
Frankland V. L., James A. D., Carrillo-Sánchez J. D., Mangan T. P., Willacy K., Poppe A. R., Plane J. M. C., 2016, Icarus, 278, 88
Fulle M., 1992, Nature, 359, 42
Fulle M. et al., 2015, ApJ, 802, L12

Downloaded from https://academic.oup.com/mnras/article-abstract/490/2/2421/5584353 by University of California School of Law (Boalt Hall) user on 29 October 2019

Fulle M. et al., 2017, MNRAS, 469, S45
Grigorieva A., Thébault P., Artymowicz P., Brandeker A., 2007, A&A, 475, 755
Grün E. et al., 1997, Icarus, 129, 270
Gustafson B. A. S., 1994, Annu. Rev. Earth Planet. Sci., 22, 553
Hahn G., Lagerkvist C.-I., Karlsson O., Oja T., Stoss R. M., 2006, Astron. Nachr., 327, 17
Hahn J. M., Zook H. A., Cooper B., Sunkara B., 2002, Icarus, 158, 360
Han D., Poppe A. R., Piquette M., Grün E., Horányi M., 2011, Geophys. Res. Lett., 38, L24102
Hanner M. S., Weinberg J. L., DeShields L. M., II, Green B. A., Toller G. N., 1974, J. Geophys. Res., 79, 3671
Hartmann W. K., Tholen D. J., Meech K. J., 1990, Icarus, 83, 1
Hillier J. K. et al., 2007, Icarus, 190, 643
Horner J., Evans N. W., Bailey M. E., 2004, MNRAS, 354, 798
Horányi M. et al., 2008, Space Sci. Rev., 140, 387
Hosek M. W., Jr, Blaauw R. C., Cooke W. J., Suggs R. M., 2013, AJ, 145, 122
Hsu H.-W., Kempf S., Jackman C. M., 2010, Icarus, 206, 653
Hsu H.-W., Kempf S., Postberg F., Trieloff M., Burton M., Roy M., Moragas-Klostermeyer G., Srama R., 2011, J. Geophys. Res., 116, A08213
Humes D. H., 1980, J. Geophys. Res., 85, 5841
Jewitt D., 2009, AJ, 137, 4296
Jones J., 1995, MNRAS, 275, 773
Kelsall T. et al., 1998, ApJ, 508, 44
Kempf S. et al., 2008, Icarus, 193, 420
Kobayashi H., Kimura J., Yamamoto S., Watanabe S., Yamamoto T., 2010, Earth Planets Space, 62, 57
Kobayashi H., Watanabe S., Kimura H., Yamamoto T., 2009, Icarus, 201, 395
Kowal C. T., Liller W., Marsden B. G., 1979, in Duncombe R. L., ed., Proc. IAU Symp. Vol. 81, Dynamics of the Solar System. Reidel, Dordrecht, p. 245
Krüger H., Krivov A. V., Grün E., 2000, Planet. Space Sci., 48, 1457
Krüger H. et al., 1999, Planet. Space Sci., 47, 85
Kulyk I., Korsun P., Rousselot P., Afanasiev V., Ivanova O., 2016, Icarus, 271, 314
Landgraf M., Liou J.-C., Zook H. A., Grün E., 2002, AJ, 123, 2857
Levison H. F., Duncan M. J., 1997, Icarus, 127, 13
Lisse C. M., Kraemer K. E., Nuth J. A., III, Li A., Joswiak D., 2007, Icarus, 187, 69
Lisse C. M. et al., 2006, Science, 313, 635
Love S. G., Joswiak D. J., Brownlee D. E., 1994, Icarus, 111, 227
Lyons J. R., 1995, Science, 267, 648
Malaspina D. M., Horányi M., Zaslavsky A., Goetz K., Wilson L. B., III, Kersten K., 2014, Geophys. Res. Lett., 41, 266
Ma Y., Williams I. P., Chen W., 2002, MNRAS, 337, 1081
Mazzotta Epifani E., Dall'Ora M., Perna D., Palumbo P., Colangeli L., 2011, MNRAS, 415, 3097
Mazzotta Epifani E., Perna D., Dotto E., Palumbo P., Dall'Ora M., Micheli M., Ieva S., Perozzi E., 2017, A&A, 597, A59
Mazzotta Epifani E. et al., 2014, A&A, 565, A69
Meech K. J. et al., 2009, Icarus, 201, 719
Moses, J. I.and Poppe, A. R.(2017) Icarus, 297, 33
Moses J. I., Bass S. F., 2000, J. Geophys. Res., 105, 7013
Moses J. I., Lellouch E., Bézard B., Gladstone G. R., Feuchtgruber H., Allen M., 2000, Icarus, 145, 166
Mukai T., Schwehm G., 1981, A&A, 95, 373
Neslušan L., Tomko D., Ivanova O., 2017, Contr. Astron. Obser. Skalneté Pleso, 47, 7
Nesvorný D., Jenniskens P., Levison H. F., Bottke W. F., Vokrouhlický D., Gounelle M., 2010, ApJ, 713, 816
Petit J. et al., 2011, AJ, 142, 131
Petrie S., 2004, Icarus, 171, 199
Piquette M. et al., 2019, Icarus, 321, 116
Poppe A., James D., Jacobsmeyer B., Horányi M., 2010, Geophys. Res. Lett., 37, L11101
Poppe A. R., 2016, Icarus, 264, 369
Poppe A. R. et al., 2019, ApJ, 881, L12
Poulet F., Cuzzi J. N., 2002, Icarus, 160, 350
Rowan-Robinson M., May B., 2013, MNRAS, 429, 2894
Schambeau C. A., Fernández Y. R., Lisse C. M., Samarasinha N., Woodney L. M., 2015, Icarus, 260, 60
Spahn F. et al., 2006, Science, 311, 1416
Srama R. et al., 2004, Space Sci. Rev., 114, 465
Srama R. et al., 2006, Planet. Space Sci., 54, 967
Sremčevič M., Krivov A. V., Krüger H., Spahn F., 2005, Planet. Space Sci., 53, 625
Stern S. A., 1996, A&A, 310, 999
Szalay J. R., Piquette M., Horányi M., 2013, Earth Planets Space, 65, 1145
Tiscareno M. S., Malhotra R., 2003, AJ, 126, 3122
Verbiscer A. J., Skrutskie M. F., Hamilton D. P., 2009, Nature, 461, 1098
Vitense C., Krivov A. V., Kobayashi H., Löhne T., 2012, A&A, 540, A30
Volk K., Malhotra R., 2013, Icarus, 224, 66
Wehry A., Mann I., 1999, A&A, 341, 296
Yamamoto S., Mukai T., 1998, A&A, 329, 785
Zook H. A., Berg O. E., 1975, Planet. Space Sci., 23, 183

This paper has been typeset from a TEX/LATEX file prepared by the author.

Downloaded from https://academic.oup.com/mnras/article-abstract/490/2/2421/5584353 by University of California School of Law (Boalt Hall) user on 29 October 2019